

Correction of Fragile X Syndrome in Mice

Gül Dölen,^{1,2} Emily Osterweil,¹ B.S. Shankaranarayana Rao,³ Gordon B. Smith,¹ Benjamin D. Auerbach,¹ Sumantra Chattarji,⁴ and Mark F. Bear^{1,*}

¹Howard Hughes Medical Institute, The Picower Institute for Learning and Memory, Department of Brain and Cognitive Sciences, Massachusetts Institute of Technology, Cambridge, MA 02139, USA

²Department of Neuroscience, Brown Medical School and the Division of Biology and Medicine, Providence, RI 02912, USA

³Department of Neurophysiology, National Institute of Mental Health and Neuroscience, Bangalore 560 002, India

⁴National Center for Biological Sciences, Tata Institute of Fundamental Research, Bangalore 560 002, India

*Correspondence: mbear@mit.edu

DOI 10.1016/j.neuron.2007.12.001

SUMMARY

Fragile X syndrome (FXS) is the most common form of heritable mental retardation and the leading identified cause of autism. FXS is caused by transcriptional silencing of the *FMR1* gene that encodes the fragile X mental retardation protein (FMRP), but the pathogenesis of the disease is unknown. According to one proposal, many psychiatric and neurological symptoms of FXS result from unchecked activation of mGluR5, a metabotropic glutamate receptor. To test this idea we generated *Fmr1* mutant mice with a 50% reduction in mGluR5 expression and studied a range of phenotypes with relevance to the human disorder. Our results demonstrate that mGluR5 contributes significantly to the pathogenesis of the disease, a finding that has significant therapeutic implications for fragile X and related developmental disorders.

INTRODUCTION

Despite progress understanding the etiology of fragile X, it is still unknown how disruption of brain function by the *FMR1* mutation leads to a devastating syndrome that includes altered neural development, cognitive impairment, childhood epilepsy, and autism (Bernardet and Crusio, 2006). There is no treatment for fragile X syndrome (FXS), and the prospects for therapy by gene replacement are not promising (Peier et al., 2000). Future therapeutic approaches must therefore be based on a more complete understanding of the basic pathogenesis of the disease.

FMRP is enriched postsynaptically in the brain, particularly at synapses that use the major excitatory neurotransmitter glutamate, so much attention has been focused on synaptic dysfunction in FXS. Recently a “metabotropic glutamate receptor (mGluR) theory” of fragile X pathogenesis was proposed (Bear et al., 2004), based on the following four observations: (1) FMRP can function as a repressor of mRNA translation at synapses (Brown et al., 2001; Qin et al., 2005); (2) synaptic protein synthesis is stimulated

potently by activation of group 1 (Gp1) mGluRs, comprising mGluR1 and mGluR5 (Weiler and Greenough, 1993); (3) many of the lasting consequences of activating Gp1 mGluRs depend on synaptic mRNA translation (Huber et al., 2000; Karachot et al., 2001; Merlin et al., 1998; Raymond et al., 2000; Vanderklisch and Edelman, 2002; Zho et al., 2002); and (4) in the absence of FMRP, several protein synthesis-dependent consequences of activating mGluRs are exaggerated (Chuang et al., 2005; Hou et al., 2006; Huber et al., 2002; Koekkoek et al., 2005). Together, these findings have led to the idea that FMRP and Gp1 mGluRs normally work in functional opposition, and that in the absence of FMRP, unchecked mGluR-dependent protein synthesis leads to the pathogenesis of FXS (Figure S1 available online).

The appeal of the mGluR theory stems from its simplicity and the potentially profound therapeutic implication—that downregulating Gp1 mGluR signaling could correct multiple symptoms of FXS. However, the theory remains controversial. To date, the strongest evidence in favor of the mGluR theory (McBride et al., 2005; Tucker et al., 2006) has been indirect, relying on drug treatments in non-mammalian species with mGluR orthologs coupled to different signaling cascades than mammalian Gp1 mGluRs (Bjarnadottir et al., 2005). It has been shown in fragile X knockout mice that acute administration of MPEP [2-methyl-6-(phenylethynyl)-pyridine], an mGluR5 antagonist, can reversibly suppress seizure phenotypes (Chuang et al., 2005; Yan et al., 2005). However, in addition to off-target activity of MPEP (Heidbreder et al., 2003; Lea and Faden, 2006), interpretation of this finding is complicated by the fact that the drug is anticonvulsant in wild-type mice as well. Thus, it remains to be established if chronic downregulation of Gp1 mGluR signaling can correct altered development in fragile X, as predicted by the mGluR theory. In the current study, we used a genetic strategy to definitively address this critical question.

RESULTS

Rescue Strategy and Rationale

Because both the human *FMR1* and *GRM5* genes have functional homologs in the mouse (*Fmr1* and *Grm5*), we were able to generate *Fmr1* knockout mice with reduced

expression of mGluR5, the major Gp1 mGluR in the fore-brain. By crossing two mutant lines, the functional relationship between two protein products can be examined; genetic “rescue” occurs when single mutant phenotypes are attenuated in the double mutant. The power of this approach in the murine model is two-fold: (1) it is a precise and selective method to reduce mGluR5 function, and (2) it permits analysis of diverse phenotypes across many developmental time points, using a variety of experimental methods both in vitro and in vivo. In addition, unlike simpler genetically modifiable organisms, endophenotypes identified in this mammalian model not only can serve to establish genetic interaction, but also may bear direct relation to the phenotype in humans with the disease.

Fmr1 mutant mice (The Dutch-Belgian Fragile X Consortium, 1994) were crossed with *Grm5* mutant mice (Lu et al., 1997) to produce *Fmr1* knockout animals with a selective reduction in mGluR5 expression (Figure S2). To increase the therapeutic relevance, we concentrated on animals with a 50% reduction in mGluR5 rather than a complete knockout (which impairs brain function [Jia et al., 1998; Lu et al., 1997]). Littermates with four different genotypes were created in our cross: wild-type [*Fmr1* (+/Y) *Grm5* (+/+)], *Fmr1* knockout [*Fmr1* (–/Y) *Grm5* (+/+)], *Grm5* heterozygote [*Fmr1* (+/Y) *Grm5* (+/–)], and the knockout/heterozygote cross [*Fmr1* (–/Y) *Grm5* (+/–)]; these animals are termed WT, KO, HT, and CR, respectively. In all crossings, animals were on the C57Bl/6J clonal background.

The key question that we address in this study is if a reduction of mGluR5 expression will correct diverse fragile X mutant phenotypes, as predicted by the mGluR theory (Figure S1). Our genetic rescue strategy rests on the assumption that the FMRP-regulated “readout” of mGluR5 activation is modulated by *Grm5* gene dosage. One FMRP-regulated consequence of mGluR5 activation is hippocampal long-term synaptic depression (LTD), which is approximately doubled in the KO (Huber et al., 2002). It had already been established that there is a significant effect of mGluR5 expression level on LTD in the C57Bl/6J WT background (Huber et al., 2001), and we confirmed in the present study that a 50% reduction in mGluR5 protein expression also significantly reduces LTD in the *Fmr1* KO background (Figure S2). We therefore went on to examine diverse phenotypes with relevance to the human disorder, including experience-dependent cortical development, hippocampus-dependent memory, altered body growth, seizure, and postpubertal macroorchidism. All analyses of these mice were performed “blind,” without experimenter knowledge of the genotype. Note that, in each experiment, three outcomes were possible: the reduced *Grm5* gene dosage could ameliorate, exacerbate, or have no effect on *Fmr1* mutant phenotypes.

Altered Ocular Dominance Plasticity in *Fmr1* KO Mice Is Rescued by Reducing mGluR5 Expression

Ocular dominance (OD) plasticity in visual cortex, elicited by temporary monocular deprivation (MD), is the classic example of how experience modifies the brain during critical pe-

riods of development. Here, we use this paradigm to study the interaction of genes and environment in a disease model.

Visually evoked potentials (VEPs) were recorded in the visual cortex of awake mice (Figure 1A), as described previously (Frenkel and Bear, 2004). We initially assessed absolute levels of visual responsiveness across genotypes on postnatal day (P) 28 and found no difference (Figure 1B). Additional mice were studied before and after MD begun on P28. Previous studies using the chronic VEP method have shown how visual responses evolve during the course of MD (Figure S3). Closure of the contralateral eyelid initially causes depression of responses to the deprived (contralateral)-eye (apparent at 3 days MD), followed by potentiation of nondeprived (ipsilateral)-eye responses (apparent by 7 days MD) (Frenkel and Bear, 2004). Because they are recorded chronically, changes in VEPs for each animal can be conveniently described by two values: the fractional change from baseline in contralateral-eye response, and the fractional change from baseline in the ipsilateral-eye response. For reference, average effects (\pm SEM) of 3 and 7 days of MD in WT mice from a previous study (Frenkel and Bear, 2004) appear in Figure S3.

In the current study we also found that the response to 3 days MD in WT mice was dominated by deprived-eye depression, as expected. In KO littermates, however, the response to brief MD was characterized by substantial open-eye potentiation, reminiscent of what happens in WT mice after longer periods of MD. On the other hand, the HT mice showed a “hypoplastic” response to MD, as they lacked significant deprived-eye depression. However, crossing the two mutant mice resulted in a phenotype very similar to WT that was again dominated by deprived-eye depression (Figure 1C).

Plots of the average (\pm SEM) fractional changes after 3 days MD in the four genotypes are shown in Figure 1D. The KO mice displayed increased plasticity compared to the WT (MANOVA WT:KO, $p = 0.011$); HT mice displayed diminished plasticity compared to WT (MANOVA WT:HT, $p = 0.013$); CR mice showed a rescue of the KO phenotype and were not significantly different from WT (MANOVA WT:CR, $p = 0.8268$, KO:CR $p = 0.037$, HT:CR $p = 0.161$).

Since the KO and HT mutations affected OD plasticity in opposite directions, one could question whether the CR phenotype reflects rescue or the simple addition of two independent effects. However, a compound phenotype would be the absence of deprived-eye depression (the effect of reducing mGluR5) and an exaggeration of open-eye potentiation (the effect of reducing FMRP). Instead, we observe a phenotype in the CR mice that is significantly different from KO mice, and not significantly different from WT. Thus, reducing mGluR5 by 50% corrects the defect in plasticity caused by the absence of FMRP.

Density of Dendritic Spines on Cortical Pyramidal Neurons Is Increased in *Fmr1* KO and Rescued by Reducing mGluR5 Expression

Abnormalities in dendritic spines, the major targets of excitatory synapses in the brain, have long been associated

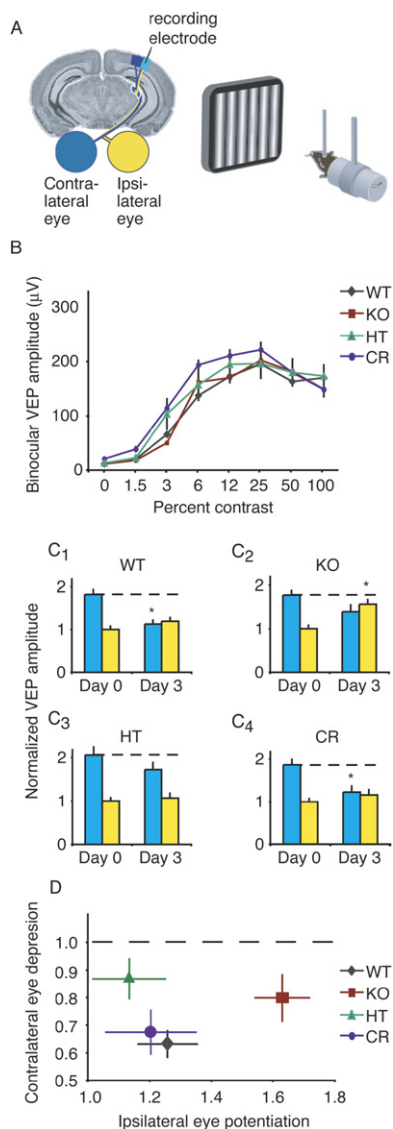


Figure 1. Genetic Rescue of OD Plasticity Phenotype in FXS

(A) Schematic of the mouse visual pathway and position of the recording electrode in primary visual cortex.

(B) Absolute VEP amplitudes recorded during binocular viewing across contrasts (0–100%, square reversing at 1 Hz, 0.05 cycles/degree). No significant differences across genotypes ($n = 46$ WT, $n = 33$ KO, $n = 8$ HT, $n = 20$ CR hemispheres, MANOVA $p = 0.0868$).

(C) Effect of 3 day MD on VEP amplitude (data expressed as mean \pm SEM, normalized to day 0 ipsilateral eye value). (C₁) WT mice ($n = 19$). Note significant deprived eye depression. (C₂) KO mice ($n = 18$). Note significant open eye potentiation. (C₃) HT mice ($n = 16$). Note absence of deprived eye depression. (C₄) CR mice ($n = 13$). Note rescue of KO phenotype. Post hoc Student's *t* tests: *Significantly different from baseline (day 0).

(D) Plots (mean \pm SEM) of the fractional change in open and deprived eye responses after 3 day MD show rescue of the KO phenotype in CR mice.

with various forms of human mental retardation, including FXS. The increased spine density phenotype observed in humans has been recapitulated in the *Fmr1* KO mouse

(reviewed by Grossman et al. [2006]). Because one protein synthesis-dependent consequence of activating Gp1 mGluRs on cortical neurons in vitro is an increase in the density of long, thin spines (Vanderklish and Edelman, 2002), we hypothesized that FMRP and mGluR5 antagonistically regulate dendritic spine density in vivo.

We chose to examine this question in layer 3 pyramidal neurons of binocular visual cortex at P30, since we had established that OD plasticity at this age was altered in the *Fmr1* KO mice. Dendritic spine density was analyzed separately in apical and basal branches across the four genotypes, using the Golgi-Cox silver staining method (Figure 2A). We observed a highly significant increase in total dendritic spine density in the KO, readily apparent as a rightward shift in the cumulative probability histogram (Figure 2B). Reducing mGluR5 expression had no effect on spine density in the HT mice, but the fragile X phenotype was completely rescued in the CR mice (apical Kruskal-Wallis test, $p < 0.0001$; Kolmogorov-Smirnov test, WT:KO $p < 0.0001$, WT:HT $p = 0.3920$, CR:WT $p = 0.4407$, CR:KO $p < 0.0001$; basal Kruskal-Wallis test, $p < 0.0001$; Kolmogorov-Smirnov test WT:KO $p < 0.0001$, WT:HT $p > 0.9999$, CR:WT $p > 0.9999$, CR:KO $p < 0.0001$).

We also performed a segmental analysis of spine density across the four genotypes. Consistent with previous observations, we observed an inverted U-shaped distribution of synapses in both apical and basal branches across all genotypes. However, as shown in Figure 2C, the density of spines was uniformly increased in the *Fmr1* KO and rescued in the CR (repeated-measures ANOVA: apical distance $p < 0.0001$, apical distance \times genotype $p < 0.0001$, apical genotype $p < 0.0001$, basal distance $p < 0.0001$, basal distance \times genotype $p = 0.0181$, basal genotype $p < 0.0001$; ANOVA genotype: apical, basal, 10–100, in 10 μ m segments $p < 0.0001$; unpaired Student's *t* tests apical, basal, 10–100, in 10 μ m segments WT:KO $p < 0.05$, WT:HT $p > 0.05$, WT:CR $p > 0.05$, KO:CR $p < 0.05$). These results suggest that neither the *Fmr1* KO phenotype nor the rescue by selective reduction in gene dosage in the CR reflects a redistribution of synapses within the segment.

Increased Basal Protein Synthesis in Hippocampus of *Fmr1* KO Mice Is Rescued by Reducing mGluR5 Expression

A previous study reported an elevated basal rate of in vivo protein synthesis in the hippocampus of *Fmr1* KO mice (Qin et al., 2005). We asked if this difference could also be observed in hippocampal slices in vitro by examining the incorporation of ³⁵S-methionine/cysteine into new protein. We observed a significant effect of genotype on protein synthesis (Figure 3A). The increased protein synthesis seen in KO hippocampus was prevented by selective reduction in mGluR5 gene dosage.

Electrophoretic separation of radiolabeled translation products (Figure 3B) suggests that increased protein synthesis in the KO is not limited to one or few predominant protein species but rather extends across a broad range

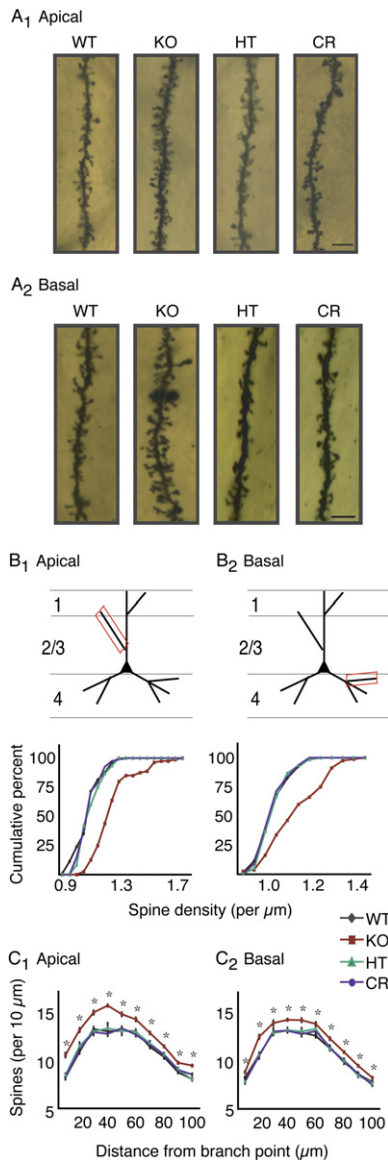


Figure 2. Genetic Rescue of Dendritic Spine Phenotype in FXS

(A) Representative images from apical (A₁) and basal (A₂) dendritic segments of layer 3 pyramidal neurons in the binocular region of primary visual cortex of all four genotypes collected at P30.

(B) Cumulative percent spines per μm in each dendritic segment; apical branches, B₁; basal branches, B₂ (n = 80 WT, 80 KO, 60 HT, 80 CR apical and basal branches, respectively). (C) Segmental analysis of spine density; number of spines per 10 μm bin, given as distance from the origin of the branch, for apical (C₁) and basal (C₂) segments across four genotypes.

of resolved molecular weights. Because the rate of protein synthesis was unaffected in the HT mice relative to WT, the rescue in the CR mice is unambiguous and does not simply reflect an offsetting decrease in synthesis of a separate pool of proteins.

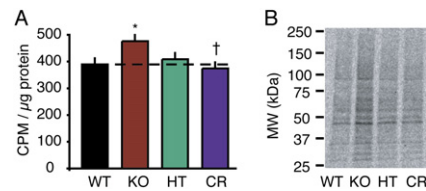


Figure 3. Genetic Rescue of Protein Synthesis Phenotype in FXS

(A) Significant differences in the levels of protein synthesis exist across genotypes in the ventral hippocampus (n = 10 samples, 5 animals per genotype). KO mice showed increased protein synthesis (mean ± SEM: WT 389 ± 33.77 cpm/μg; KO 476 ± 29.98 cpm/μg; post hoc paired Student's t test WT:KO p = 0.004). Protein synthesis levels in the HT mice were no different than WT (HT 409 ± 42.99 cpm/μg). Increased protein synthesis seen in the KO were rescued in the CR mice (CR 374 ± 50.81 cpm/μg). Post hoc paired Student's t tests: *significantly different from WT, †significantly different from KO.

(B) Representative autoradiogram shows that synthesis of many protein species is elevated in the KO compared to all other genotypes.

Inhibitory Avoidance Extinction Is Exaggerated in *Fmr1* KO Mice and Rescued by Reducing mGluR5 Expression

Although humans with FXS show mental retardation in the moderate to severe range, prior studies of cognitive performance in *Fmr1* KO mice on the C57Bl/6J clonal background have revealed only subtle deficits (Bernardet and Crusio, 2006). Consistent with these observations, we found that acquisition of one-trial inhibitory avoidance (IA), a hippocampus-dependent memory, did not differ from normal in the *Fmr1* KO mice. However, we were inspired to additionally investigate IA extinction (IAE) by a recent report that this process requires protein synthesis in the hippocampus (Power et al., 2006). We discovered that IAE is exaggerated in the *Fmr1* KO mouse and that this phenotype is corrected by reducing expression of mGluR5.

Adult mice of all four genotypes were given IA training, followed at 6 and 24 hr by IAE training (Figure 4A). For each animal, we measured the latency to enter the dark side of the box on the first trial (baseline), the latency 6 hr later (postacquisition) to assess IA memory, and again at 24 and 48 hr (post-extinction 1 and 2, respectively) to assess IAE. As shown in Figure 4B, animals of all four genotypes showed both significant IA acquisition at 6 hr and extinction by 48 hr. A global statistical test suggested that the pattern of learning across time varied across genotypes (repeated-measures ANOVA genotype × time p = 0.0239). As shown in Figures 4C–4E, these differences are likely due to extinction rather than acquisition of inhibitory avoidance. At 6 hr, there was no difference across genotypes in latency to enter (6 hr ANOVA p = 0.1525); however, at 24 hr KO mice showed significantly shorter latencies, suggesting exaggerated extinction in the absence of FMRP. This phenotype was rescued by selective reduction in mGluR5 gene dosage in the CR mice (24 hr ANOVA p = 0.0013; Student's t tests: WT:KO

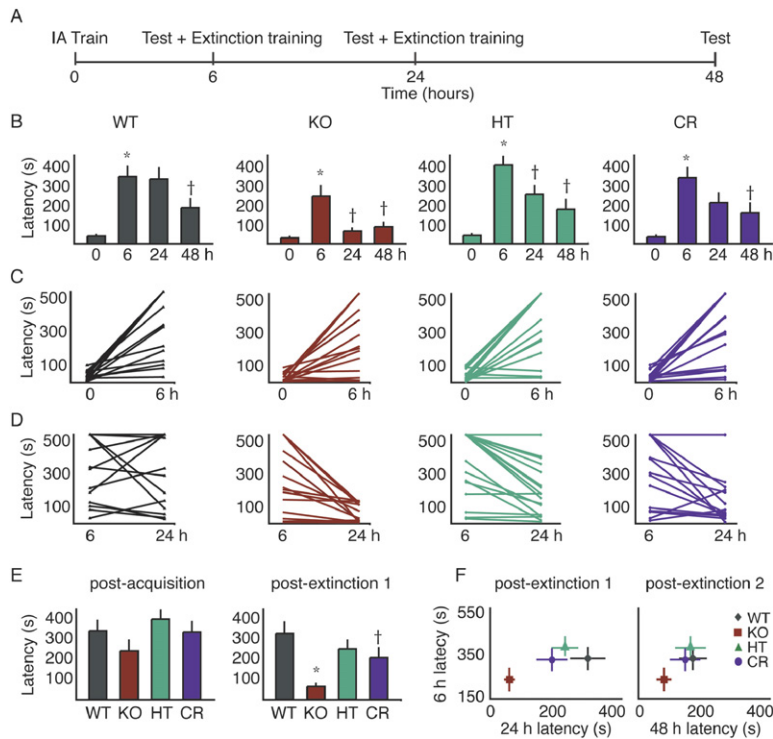


Figure 4. Genetic Rescue of Behavioral Learning and Memory Phenotype in FXS

(A) Experimental design. Animals of all four genotypes ($n = 15$ WT, $n = 15$ KO, $n = 20$ HT, $n = 17$ CR) were given IA training at time 0, and the latency to enter the dark side was measured at 6 hr. They were then given IAE training, and latency was again measured at 24 hr. Testing was followed by another round of IAE training, and latency was measured again at 48 hr. (B) Animals in all four genotypes showed significant acquisition and extinction. Post hoc Student's *t* tests: *significantly different from time 0 hr, †significantly different from time 6 hr. (C) Raw data for acquisition of IA in the four genotypes. Each line represents the change in latency to enter the dark side for one mouse (data from some mice superimpose). (D) Raw data for extinction 1 in the four genotypes. (E) Comparison of latency (mean \pm SEM) across genotypes for 6 hr time point (post-acquisition) and 24 hr time point (post-extinction 1). Post hoc Student's *t* tests: *significantly different from WT, †significantly different from KO. (F) Multivariate analysis of extinction as a function of acquisition at 24 hr time point (post-extinction 1) and 48 hr time point. Plotted are mean latencies \pm SEM.

$p < 0.0001$, WT:HT $p = 0.8251$, WT:CR $p = 0.1156$, KO:CR $p = 0.0132$.

Because the primary aim of this study is to examine genetic interaction between *Fmr1* and *Grm5*, we also performed a multivariate analysis that takes into consideration both acquisition and extinction as they vary across genotypes. As shown in Figure 4F, KO animals showed significant difference in 24 hr latency (memory retention) as it varied with 6 hr latency (memory acquisition), and this difference was rescued by the selective reduction in mGluR5 gene dosage in the CR mice (MANOVA for genotype 6:24 $p = 0.0054$, MANOVA WT:KO $p = 0.0005$, WT:HT 0.0785 , KO:CR $p = 0.0490$, WT:CR $p = 0.1863$). The difference in retention across all genotypes was not significant by 48 hr. Regardless of whether this KO phenotype reflects exaggerated extinction or diminished stability of the formed memory, there clearly is a significant genetic interaction between *Fmr1* and *Grm5*: the *Fmr1* KO phenotype is rescued by the selective reduction in mGluR5 expression.

Audiogenic Seizures and Accelerated Body Growth in *Fmr1* KO Mice Are Rescued by Reducing mGluR5 Expression

Consistent with neurological findings in fragile X patients, previous studies have shown increased seizure susceptibility in the *Fmr1* KO mouse, using both in vitro and in vivo epilepsy models (Bernardet and Crusio, 2006). We employed the audiogenic seizure (AGS) paradigm, which shows a robust phenotype in *Fmr1* KO mice and exhibits developmental changes consistent with epilepsy in

human FXS (Yan et al., 2005). Because C57Bl/6 WT mice are normally seizure resistant (Robertson, 1980), seizures in the KO mice are a specific consequence of the absence of FMRP. As shown in Table S1, significant differences in AGS susceptibility were observed across the four genotypes examined. WT and HT mice showed zero incidences of AGS, as expected, whereas 72% of the KO mice had a seizure in response to the tone (Mann-Whitney U test WT:KO $p < 0.0001$). This mutant phenotype was significantly attenuated in the CR mice (Mann-Whitney U test CR:KO $p = 0.028$). Thus, chronic reduction of mGluR5 gene dosage in KO mice produced a substantial rescue of the seizure phenotype that is caused specifically by the lack of FMRP.

Children with FXS show accelerated prepubescent growth (Loesch et al., 1995). We discovered that this phenotype is recapitulated in the KO mouse and is rescued by reducing mGluR5 gene dosage (Figure S4). At weaning (P20–21), animals from all four genotypes had similar body weights, but by P26 KO mice showed a slight (10%) but significant increase in body weight as compared to WT animals at the same age. This difference was not observed in either the HT or CR mice (ANOVA $p = 0.048$, post hoc Student's *t* tests WT:KO $p = 0.017$, KO:CR $p = 0.004$, CR:WT $p = 0.818$). The WT:KO body weight difference was maximal at P30 (~15%), when it was again rescued by a reduction in mGluR5 gene dosage in the CR mice (ANOVA $p = 0.005$, post hoc Student's *t* tests WT:KO $p = 0.020$, KO:CR $p = 0.001$, CR:WT $p = 0.555$). As in humans, the KO growth increase in mice was no longer apparent after adolescence (P45).

Macroorchidism in *Fmr1* KO Mice Is Not Rescued by Reducing mGluR5 Expression

Children with FXS (and KO mice) have dysmorphic features, including postadolescent macroorchidism. Testes express Gp1 mGluRs (Storto et al., 2001), so we wondered if this phenotype might also be rescued in our CR mice. Postadolescent testicular weight was increased by 24% in KO mice compared to WT ($p < 0.0004$; Student's *t* test); however, there was no rescue of this phenotype in the CR mice (Figure S5). To investigate if the absence of rescue was a matter of gene dosage, we generated KO mice that had a complete absence of mGluR5 [*Fmr1* ($-/-$) *Grm5* ($-/-$), dKO]. Again, however, there was no rescue of the testicular phenotype.

DISCUSSION

The goal of this study was to test a key prediction of the mGluR theory—that aspects of FXS can be corrected by downregulating signaling through group 1 mGluRs (Bear et al., 2004). Each analysis was designed to examine a different dimension of the disorder in mice with relevance to the human syndrome, ranging from the cognitive to the somatic. The experiments assayed dysfunction in very different neural circuits; and for each, three outcomes were possible: amelioration, exacerbation, or persistence of *Fmr1* mutant phenotypes in mice with reduced expression of mGluR5. Thus, it is remarkable that by reducing mGluR5 gene dosage by 50%, we were able to bring multiple, widely varied fragile X phenotypes significantly closer to normal.

A novel aspect of the current study was the use of OD plasticity as an *in vivo* assay of how experience-dependent synaptic modification is altered by the loss of FMRP. MD sets in motion a sequence of synaptic changes in visual cortex, characterized by a rapid and persistent loss of responsiveness to the deprived eye and a slower compensatory increase in responsiveness to the nondeprived eye (Frenkel and Bear, 2004). Because MD triggers mechanisms of synaptic depression and potentiation, as well as homeostatic adaptations to an altered environment, OD plasticity is a particularly rich paradigm for understanding the interactions of genes and experience. The intersecting trends of using mice to study OD plasticity mechanisms and to model human diseases provided the opportunity to use this paradigm to get a more precise understanding of how development goes awry in a genetic disorder.

Previous work suggested that Gp1 mGluR signaling is highest in visual cortex during the period of maximal synaptic plasticity (Dudek and Bear, 1989), and the current findings strongly suggest an important role for mGluR5 in OD plasticity. Although more experiments will be required to pinpoint this role, an obvious clue comes from the genetic interaction with *Fmr1*. FMRP can act as a translational suppressor (Brown et al., 2001; Qin et al., 2005), and OD plasticity, like many forms of persistent synaptic modification, requires protein synthesis (Taha and Stryker, 2002). Thus, our findings suggest the intriguing

hypothesis that the rate of plasticity in visual cortex is determined by the level of activity-dependent protein synthesis, which is stimulated by mGluR5 and inhibited by FMRP. Consistent with this model, the phenotype in *Fmr1* KO mice appears to reflect “hyperplasticity,” since 3 days of MD yielded effects on VEPs that normally require 7 days. This exaggerated plasticity was corrected by reducing mGluR5 expression by 50%.

Although we observed an increased spine density in the visual cortex of KO mice, there was no apparent difference in the amplitude of VEPs at P30. This discrepancy may be because VEPs were recorded in layer 4, whereas the spine measurements were made on layer 3 neurons. In any case, the clear mutant spine phenotype in layer 3 gave us the opportunity to examine if this structural defect could also be corrected by decreasing mGluR5. We observed a remarkable rescue of the fragile X spine phenotype in the CR mice, despite the fact that reducing mGluR5 expression in the HT mice had no effect on spine density. Thus, although the reduction in *Grm5* gene dosage is not sufficient to alter spine density by itself, it completely corrects the defect in fragile X mice.

Strain-specific variation has confounded previous attempts to identify a behavioral learning and memory phenotype in the *Fmr1* KO (Bernardet and Crusio, 2006). Consistent with earlier findings, we were unable to detect a significant IA deficit in the *Fmr1* KO mice on the C57BL/6 background. On the other hand, we were able to detect a difference in the rate of IA extinction that could be corrected by reducing mGluR5 expression. Because IA induces LTP of Schaffer collateral synapses in area CA1 of the hippocampus (Whitlock et al., 2006), it is tempting to speculate that IA extinction is exaggerated in *Fmr1* KO mice due, at least in part, to excessive mGluR-dependent synaptic weakening (Huber et al., 2002; Zho et al., 2002). Unbalanced LTD could account for the cognitive impairment that is the hallmark of fragile X.

Fragile X is a syndromic disorder. In addition to mental retardation, associated features of the disease in humans include childhood epilepsy, altered body growth, and postpubertal macroorchidism. In the case of epilepsy and macroorchidism, these phenotypes have been recapitulated in the mouse model (Bernardet and Crusio, 2006); however, it was previously unknown that *Fmr1* KO mice show a similar disruption in body growth. Both the body growth and AGS phenotypes were ameliorated in the CR mice; however, there was no evidence of an interaction between FMRP and mGluR5 in the control of testicle size. These results argue against a role for mGluR5 in the pathogenesis of the macroorchidism phenotype in FXS, but we cannot rule out a contribution of the other Gp1 mGluR (mGluR1).

Conclusion

Although we studied a range of phenotypes, a simple way to conceptualize the constellation of findings is that fragile X is a disorder of excess—excessive sensitivity to environmental change, synaptic connectivity, protein synthesis,

memory extinction, body growth, and excitability—and these excesses can be corrected by reducing mGluR5. Although the precise molecular basis of the interaction remains to be determined, the data show unambiguously that mGluR5 and FMRP act as an opponent pair in several functional contexts and support the theory that many CNS symptoms in fragile X are accounted for by unbalanced activation of Gp1 mGluRs. These findings have major therapeutic implications for FXS and autism (see Bear et al., 2008).

EXPERIMENTAL PROCEDURES

Animals

Fmr1 mutant mice (Jackson Labs) were crossed with *Grm5* mutants (Jackson Labs) to produce mice of four genotypes. In all crossings, animals were on the C57Bl/6J clonal background. In an effort to reduce variability due to rearing conditions, all experimental animals were bred from *Fmr1* heterozygote mothers, group housed (animals weaned to solitary housing were excluded), and maintained in a 12:12 hr light:dark cycle. Paternal genotype varied between crossings and included WT, *Grm5* HT, or *Grm5* KO.

Genotyping

See Figure S2 and the Supplemental Data.

Electrophysiology and Spine Measurements

Transverse hippocampal slices were prepared from P25–30 mice and mGluR-LTD was studied as described by Huber et al. (2001). VEP recordings and monocular deprivation were performed as previously described (Frenkel and Bear, 2004). Spines were analyzed using the Golgi-Cox method as described by Hayashi et al. (2004). Animal $n = 8$ WT, 8 KO, 6 HT, 8 CR; dendritic segment $n = 80$ WT, 80 KO, 60 HT, 80 CR apical and basal branches, respectively. All protrusions, irrespective of their morphological characteristics, were counted as spines if they were in direct continuity with the dendritic shaft. In total, 68,032 spines were counted across all four genotypes.

Inhibitory Avoidance Extinction, Metabolic Labeling, and Audiogenic Seizure

IAE experiments were performed as previously described (Power et al., 2006). Metabolic labeling experiments were similar to those described in Raymond et al. (2000). AGS experiments were performed as described by Yan et al. (2005). See Supplemental Data.

Statistical Analysis

In all cases, post hoc comparisons between genotypes were made only if global analysis indicated a statistically significant ($p < 0.05$) effect of genotype. Outliers (≥ 2 SD from the mean) were excluded. For AGS experiments, nonparametric statistics (Kruskal-Wallis, Mann-Whitney U) were used since incidence scores were bimodal (yes/no). For all other analysis, parametric tests (ANOVA, MANOVA, two-tailed paired and unpaired Student's t tests, assuming equal variance) were used. For the metabolic labeling experiments, the post hoc paired Student's t test was used to eliminate the variability due to strength of radioactive label on different experimental days and was justified by the experimental design (samples were collected with yoked, rather than randomized, controls).

Supplemental Data

The Supplemental Data for this article can be found online at <http://www.neuron.org/cgi/content/full/56/6/955/DC1/>.

ACKNOWLEDGMENTS

We are grateful to M. Shuler for helpful discussion of appropriate statistical analysis; K. Oram, C. Dudley, A. Topolszki, T. Udaka, and C. Poo for genotyping and animal care; E. Sklar for technical assistance and construction of AGS stimulus; M. Frenkel for use of previously published data; S. Meagher for administrative support; A. Kraev and J. Roder for *Grm5* genotyping protocols; K. Huber, K. Wiig, A. Govindarajan, R. Paylor, W. Chen, B. Yoon, Q. Yan, R. Bauchwitz, M. Tranfaglia, E. Klann, E. Berry-Kravis, and A. Heynen for helpful discussions. Supported by the NIMH, NICHD, National Fragile X Foundation, FRAXA, Simons Foundation. M.F.B. discloses a financial interest in Seaside Therapeutics.

Received: March 29, 2007

Revised: October 8, 2007

Accepted: December 3, 2007

Published: December 19, 2007

REFERENCES

- Bear, M.F., Huber, K.M., and Warren, S.T. (2004). The mGluR theory of fragile X mental retardation. *Trends Neurosci.* 27, 370–377.
- Bear, M.F., Dolen, G., Osterweil, E., and Nagarajan, N. (2008). Fragile X: Translation in action. *Neuropsychopharmacology* 33, 84–87.
- Bernardet, M., and Crusio, W.E. (2006). *Fmr1* KO mice as a possible model of autistic features. *ScientificWorldJournal* 6, 1164–1176.
- Bjarnadottir, T.K., Schiöth, H.B., and Fredriksson, R. (2005). The phylogenetic relationship of the glutamate and pheromone G-protein-coupled receptors in different vertebrate species. *Ann. N Y Acad. Sci.* 1040, 230–233.
- Brown, V., Jin, P., Ceman, S., Darnell, J.C., O'Donnell, W.T., Tenenbaum, S.A., Jin, X., Feng, Y., Wilkinson, K.D., Keene, J.D., et al. (2001). Microarray identification of FMRP-associated brain mRNAs and altered mRNA translational profiles in fragile X syndrome. *Cell* 107, 477–487.
- Chuang, S.C., Zhao, W., Bauchwitz, R., Yan, Q., Bianchi, R., and Wong, R.K. (2005). Prolonged epileptiform discharges induced by altered group I metabotropic glutamate receptor-mediated synaptic responses in hippocampal slices of a fragile X mouse model. *J. Neurosci.* 25, 8048–8055.
- Dudek, S.M., and Bear, M.F. (1989). A biochemical correlate of the critical period for synaptic modification in the visual cortex. *Science* 246, 673–675.
- The Dutch-Belgian Fragile X Consortium. (1994). *Fmr1* knockout mice: A model to study fragile X mental retardation. *Cell* 78, 23–33.
- Frenkel, M.Y., and Bear, M.F. (2004). How monocular deprivation shifts ocular dominance in visual cortex of young mice. *Neuron* 44, 917–923.
- Grossman, A.W., Aldridge, G.M., Weiler, I.J., and Greenough, W.T. (2006). Local protein synthesis and spine morphogenesis: Fragile X syndrome and beyond. *J. Neurosci.* 26, 7151–7155.
- Hayashi, M.L., Choi, S.Y., Rao, B.S., Jung, H.Y., Lee, H.K., Zhang, D., Chattarji, S., Kirkwood, A., and Tonegawa, S. (2004). Altered cortical synaptic morphology and impaired memory consolidation in forebrain-specific dominant-negative PAK transgenic mice. *Neuron* 42, 773–787.
- Heidbreder, C.A., Bianchi, M., Lacroix, L.P., Faedo, S., Perdon, E., Remelli, R., Cavanni, P., and Crespi, F. (2003). Evidence that the metabotropic glutamate receptor 5 antagonist MPEP may act as an inhibitor of the norepinephrine transporter in vitro and in vivo. *Synapse* 50, 269–276.
- Hou, L., Antion, M.D., Hu, D., Spencer, C.M., Paylor, R., and Klann, E. (2006). Dynamic translational and proteasomal regulation of fragile X

- mental retardation protein controls mGluR-dependent long-term depression. *Neuron* 51, 441–454.
- Huber, K.M., Kayser, M.S., and Bear, M.F. (2000). Role for rapid dendritic protein synthesis in hippocampal mGluR-dependent long-term depression. *Science* 288, 1254–1257.
- Huber, K.M., Roder, J.C., and Bear, M.F. (2001). Chemical induction of mGluR5- and protein synthesis-dependent long-term depression in hippocampal area CA1. *J. Neurophysiol.* 86, 321–325.
- Huber, K.M., Gallagher, S.M., Warren, S.T., and Bear, M.F. (2002). Altered synaptic plasticity in a mouse model of fragile X mental retardation. *Proc. Natl. Acad. Sci. USA* 99, 7746–7750.
- Jia, Z., Lu, Y., Henderson, J., Taverna, F., Romano, C., Abramow-Newerly, W., Wojtowicz, J.M., and Roder, J. (1998). Selective abolition of the NMDA component of long-term potentiation in mice lacking mGluR5. *Learn. Mem.* 5, 331–343.
- Karachot, L., Shirai, Y., Vigot, R., Yamamori, T., and Ito, M. (2001). Induction of long-term depression in cerebellar Purkinje cells requires a rapidly turned over protein. *J. Neurophysiol.* 86, 280–289.
- Koekkoek, S.K., Yamaguchi, K., Milojkovic, B.A., Dortland, B.R., Ruigrok, T.J., Maex, R., De Graaf, W., Smit, A.E., VanderWerf, F., Bakker, C.E., et al. (2005). Deletion of FMR1 in Purkinje cells enhances parallel fiber LTD, enlarges spines, and attenuates cerebellar eyelid conditioning in Fragile X syndrome. *Neuron* 47, 339–352.
- Lea, P.M., IV, and Faden, A.I. (2006). Metabotropic glutamate receptor subtype 5 antagonists MPEP and MTEP. *CNS Drug Rev.* 12, 149–166.
- Loesch, D.Z., Huggins, R.M., and Hoang, N.H. (1995). Growth in stature in fragile X families: A mixed longitudinal study. *Am. J. Med. Genet.* 58, 249–256.
- Lu, Y.M., Jia, Z., Janus, C., Henderson, J.T., Gerlai, R., Wojtowicz, J.M., and Roder, J.C. (1997). Mice lacking metabotropic glutamate receptor 5 show impaired learning and reduced CA1 long-term potentiation (LTP) but normal CA3 LTP. *J. Neurosci.* 17, 5196–5205.
- McBride, S.M., Choi, C.H., Wang, Y., Liebelt, D., Braunstein, E., Ferreiro, D., Sehgal, A., Siwicki, K.K., Dockendorff, T.C., Nguyen, H.T., et al. (2005). Pharmacological rescue of synaptic plasticity, courtship behavior, and mushroom body defects in a *Drosophila* model of fragile X syndrome. *Neuron* 45, 753–764.
- Merlin, L.R., Bergold, P.J., and Wong, R.K. (1998). Requirement of protein synthesis for group I mGluR-mediated induction of epileptiform discharges. *J. Neurophysiol.* 80, 989–993.
- Peier, A.M., McIlwain, K.L., Kenneson, A., Warren, S.T., Paylor, R., and Nelson, D.L. (2000). (Over)correction of FMR1 deficiency with YAC transgenics: Behavioral and physical features. *Hum. Mol. Genet.* 9, 1145–1159.
- Power, A.E., Berlau, D.J., McGaugh, J.L., and Steward, O. (2006). Anisomycin infused into the hippocampus fails to block “reconsolidation” but impairs extinction: The role of re-exposure duration. *Learn. Mem.* 13, 27–34.
- Qin, M., Kang, J., Burlin, T.V., Jiang, C., and Smith, C.B. (2005). Post-adolescent changes in regional cerebral protein synthesis: An in vivo study in the FMR1 null mouse. *J. Neurosci.* 25, 5087–5095.
- Raymond, C.R., Thompson, V.L., Tate, W.P., and Abraham, W.C. (2000). Metabotropic glutamate receptors trigger homosynaptic protein synthesis to prolong long-term potentiation. *J. Neurosci.* 20, 969–976.
- Robertson, H.A. (1980). Audiogenic seizures: Increased benzodiazepin receptor binding in a susceptible strain of mice. *Eur. J. Pharmacol.* 66, 249–252.
- Storto, M., Sallèse, M., Salvatore, L., Poulet, R., Condorelli, D.F., Dell’Albani, P., Marcello, M.F., Romeo, R., Piomboni, P., Barone, N., et al. (2001). Expression of metabotropic glutamate receptors in the rat and human testis. *J. Endocrinol.* 170, 71–78.
- Taha, S., and Stryker, M.P. (2002). Rapid ocular dominance plasticity requires cortical but not geniculate protein synthesis. *Neuron* 34, 425–436.
- Tucker, B., Richards, R.I., and Lardelli, M. (2006). Contribution of mGluR and Fmr1 functional pathways to neurite morphogenesis, craniofacial development and fragile X syndrome. *Hum. Mol. Genet.* 15, 3446–3458.
- Vanderklish, P.W., and Edelman, G.M. (2002). Dendritic spines elongate after stimulation of group 1 metabotropic glutamate receptors in cultured hippocampal neurons. *Proc. Natl. Acad. Sci. USA* 99, 1639–1644.
- Weiler, I.J., and Greenough, W.T. (1993). Metabotropic glutamate receptors trigger postsynaptic protein synthesis. *Proc. Natl. Acad. Sci. USA* 90, 7168–7171.
- Whitlock, J.R., Heynen, A.J., Shuler, M.G., and Bear, M.F. (2006). Learning induces long-term potentiation in the hippocampus. *Science* 313, 1093–1097.
- Yan, Q.J., Rammal, M., Tranfaglia, M., and Bauchwitz, R.P. (2005). Suppression of two major Fragile X Syndrome mouse model phenotypes by the mGluR5 antagonist MPEP. *Neuropharmacology* 49, 1053–1066.
- Zho, W.M., You, J.L., Huang, C.C., and Hsu, K.S. (2002). The group I metabotropic glutamate receptor agonist (S)-3,5-dihydroxyphenylglycine induces a novel form of depotentiation in the CA1 region of the hippocampus. *J. Neurosci.* 22, 8838–8849.

Neuron, Volume 56

Supplemental Data

Correction of Fragile X Syndrome in Mice

Gül Dölen, Emily Osterweil, B.S. Shankaranarayana Rao, Gordon B. Smith, Benjamin D. Auerbach, Sumantra Chattarji, and Mark F. Bear

Supplemental Experimental Procedures

Genotyping

Screening for the presence or absence of the wild-type allele on the *Fmr1* locus was performed using primer S1 (5' GTG GTT AGC TAA AGT GAG GAT GAT 3') and S2 (5' CAG GTT TGT TGG GAT TAA CAG ATC 3') and the knockout allele using primer M2 (5' ATC TAG TCA TGC TAT GGA TAT CAG C 3') and N2 (5' GTG GGC TCT ATG GCT TCT GAG G 3'). For the *Fmr1* locus the following PCR program was used: 95 °C for 5 min; 34 PCR cycles were performed composed of 30 sec at 95 °C, 30 sec at 61 °C, and 1min at 72°C. KO and WT PCR reactions were run separately; the reaction products were then combined and electrophoresed on a 1.5% agarose gel [WT: 465 BP (S1/S2); KO: 800 BP (M2/N2)]. Screening for the presence or absence of the knockout allele on the *Grm5* locus was performed using primer P (5' AGG GGA GGA GTA GAA GGT GGC GCG A 3') and F (5' GCT CAC ATG CCA GGT GAC ATT ATT ATT GGA 3') and the wild-type allele using F (see above) and R (5' CCA TGC TAG TTG CAG AGT AAG CAA TCT GAG GT 3'). For the *Grm5* locus the following PCR program was used: 95 °C for 5 min; 34 PCR cycles were performed composed of 30 sec at 95 °C, 55 sec at 61 °C, and 1min at 72 °C. KO and WT PCR reactions were run separately; the reaction products were then combined and electrophoresed on a 1.5% agarose gel [WT: 445 BP (F/R); KO: 550 BP (F/P)]. All primers were generated by Invitrogen.

Inhibitory Avoidance Extinction

On the day before training adult mice of all four genotypes (P60-P110) were moved into the behavioral testing room. On the day of testing, animals were placed into the dark compartment of an IA training box (a two-chambered Perspex box consisting of a lighted safe side and a dark shock side separated by a trap door) for 30 seconds followed by 90 seconds in the light compartment for habituation. Following the habituation period, the door separating the two compartments was opened and animals were allowed to enter the dark compartment. Latency to enter following door opening was recorded ("baseline", time 0, 8a.m.-12p.m.); animals with baseline entrance latencies of greater than 120 seconds were excluded. After each animal stepped completely into the dark compartment with all four paws, the sliding door was closed and the animal received a single scrambled foot-shock (0.5mA, 2.0 sec) via electrified steel rods in the floor of the box. This intensity and duration of shock consistently caused animals to vocalize and jump. Animals remained in the dark compartment for 15 sec following the shock and were then returned to their home cages. Six to seven hours following IA training, mice received a retention test ("post-acquisition", time 6 hours, 2p.m.-6p.m.). During post-acquisition retention testing each animal was placed in the lit compartment as in training; after a 90 second delay, the

door opened, and the latency to enter the dark compartment was recorded (cutoff time 540 sec). For inhibitory avoidance extinction (IAE) training, animals were allowed to explore the dark compartment of the box for 200 seconds in the absence of foot-shock (animals remaining in the lit compartment after the cutoff were gently guided, using an index card, into the dark compartment); following IAE training animals were returned to their home cages. Twenty-four hours following initial IA training, mice received a second retention test (“post-extinction 1”, time 24 hours, 8a.m.-12p.m.). Animals were tested in the same way as at the six hour time point, followed by a second 200 second extinction trial in the dark side of the box; following training animals were again returned to their home cages. Forty-eight hours following avoidance training, mice received a third and final retention test (“post-extinction 2”, time 48 hours, 8a.m.-12p.m.).

Metabolic Labeling

Pilot studies indicated that the difference between WT and KO protein synthesis was most pronounced in the ventral hippocampus so all subsequent experiments were restricted to slices from this region. Briefly, 500 μ m sections were prepared from one hippocampus per animal (average age P84) using a tissue slicer (Stoelting Co.), and transferred to a custom-made incubation manifold with multiple separate inserts (15 mm diameter netwells, Electron Microscopy Sciences) suspended in carbogenated, 32.5°C ACSF (124 mM NaCl; 5 mM KCl; 1.25 mM NaH₂PO₄; 26 mM NaHCO₃; 0.8 mM MgCl₂; 1.8 mM CaCl₂; and 10 mM dextrose saturated with 95% O₂, 5% CO₂). Following a 4 hour recovery, netwells containing slices were transferred to a second manifold chamber containing 100 ml carbogenated ACSF with 11 μ Ci/ \square l ³⁵S-Met/Cys (EasyTag Express protein labeling mix, Perkin Elmer) and incubated for 1 hour. Netwells were then transferred to 12-well dish containing ice-cold dissection buffer to stop protein synthesis and remove excess ³⁵S-Met/Cys, and slices were subsequently removed and homogenized in ice-cold homogenization buffer. Samples were then incubated in Trichloroacetic acid (TCA; 10% final) for 10 minutes on ice, spun at 21,000xg, 10 minutes, 4°C, and the pellet washed with ice-cold ddH₂O. Pellets were then resolubilized in 37°C 1N NaOH, and pH adjusted with 1N HCl. For each sample, triplicate aliquots were then read with a scintillation counter (Beckman Instruments) using HiSafe 2 scintillation cocktail (Perkin Elmer), and triplicate aliquots were subjected to a protein concentration assay (Bio-Rad). These triplicate readings were averaged, and the counts per minute (CPM) obtained were divided by the CPM obtained (in triplicate) from the ³⁵S-Met/Cys ASCF used for incubation. Final data were thus expressed as incorporated CPM per μ g protein. Equal amounts of protein from each sample were subjected to SDS-PAGE and transferred to nitrocellulose membranes. Autoradiography was performed on the dried membranes. Staining with MemCode blot stain (Pierce) confirmed equal loading. One dimensional line scans were performed using the gel analyzer tool in Image J to visualize the breadth of radiolabeled species across genotypes.

Audiogenic Seizure

Animals at P19-21 (immediately following weaning) were habituated to the behavioral chamber (28x17.5x12 cm transparent plastic box) for 2 minutes prior to stimulus onset. AGS stimulus was a 125 dbSPL at 0.25 m siren (modified personal alarm, Radioshack model 49-1010, powered from a DC converter). Seizures were scored for incidence during a 5 minute stimulus presentation or until animal reached AGS endpoint (status epilepticus/ respiratory arrest/ death).

Figure S1. The mGluR theory of fragile X syndrome

(A) Activation of mGluR5 initiates a divergent signaling cascade in neurons. Considerable evidence suggests that some (but not all) lasting consequences of mGluR5 activation are (1) protein synthesis-dependent, and (2) negatively regulated by FMRP. (B) The mGluR theory of fragile X posits that the major symptoms (phenotypes) of fragile X are due to an exaggeration of those consequences of mGluR activation that are normally regulated by FMRP. Note that the theory makes no assumptions about alterations in mGluR signaling that are not regulated by FMRP. (C) The question we ask in this study is whether diverse fragile X phenotypes in the mouse model of the disease can be corrected by a 50% reduction in mGluR5 expression. The theory predicts that the effects of reducing mGluR5 should be not restricted to one or a few phenotypes, and the data support this prediction. We show that visual cortical plasticity and spine density, hippocampus-dependent inhibitory avoidance extinction and protein synthesis, auditory epileptogenesis, and prepubescent weight gain are all exaggerated in the *Fmr1* KO mouse, and all are brought significantly closer to normal by reducing mGluR5 expression by 50%.

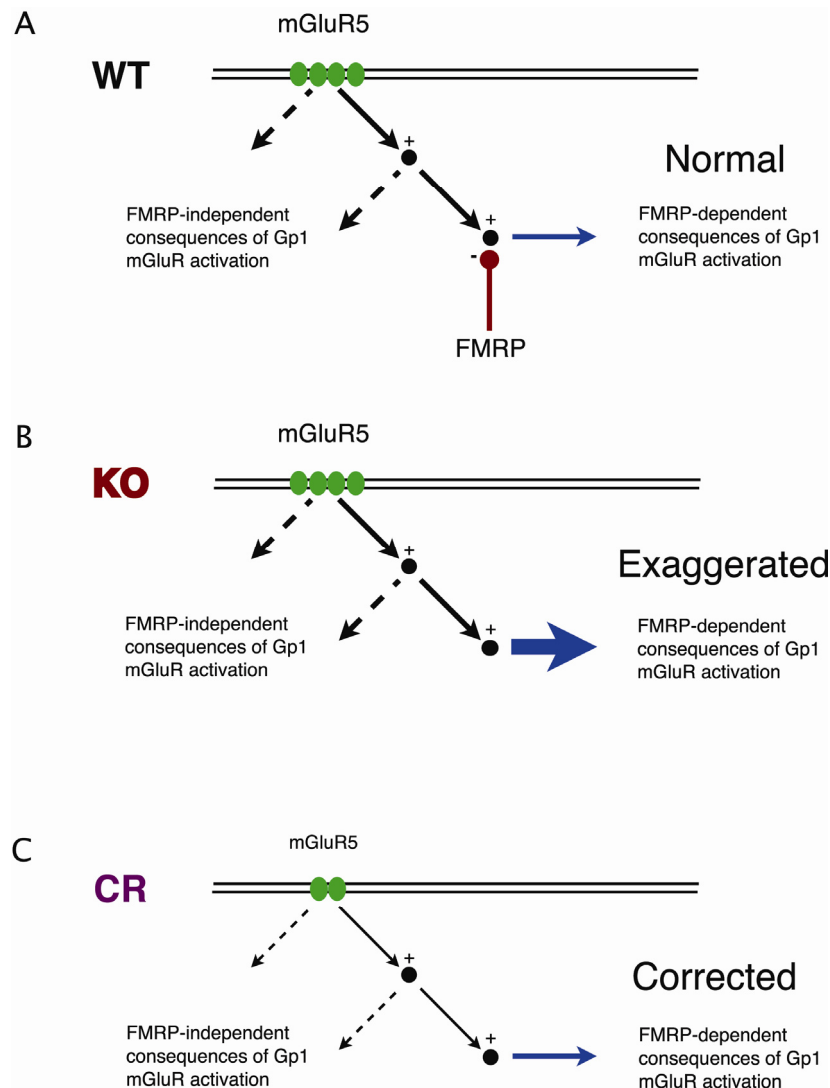


Figure S2. Generation *Fmr1* KO mice with a selective reduction of *Grm5* gene dosage

(A) *Fmr1* heterozygous females were crossed with *Grm5* heterozygous males to generate littermate male offspring of four genotypes: wild type, WT (black); *Fmr1* KO, KO (red); *Grm5* HET, HT (green); and *Fmr1* KO/*Grm5* HET, CR (purple). (B) Genotyping strategy. Screening for the presence or absence of the wild-type allele on the *Fmr1* locus on the X chromosome was performed using primer S1 (forward) and S2 (reverse) and the knockout allele using primer M2 (forward) and N2 (reverse). KO and WT PCR reactions were run separately; the reaction products were then combined and electrophoresed on a 1.5% agarose gel [*Fmr1* WT: 465 BP (S1/S2); *Fmr1* KO: 800 BP (M2/N2)]. Screening for the presence or absence of the knockout allele on the *Grm5* locus of chromosome 7 was performed using primer P (reverse) and F (forward) and the wild-type allele using F (forward) and R (reverse). KO and WT PCR reactions were run separately; the reaction products were then combined and electrophoresed on a 1.5% agarose gel [*Grm5* WT: 445 BP (F/R); *Grm5* KO: 550 BP (F/P)]. Representative gel for mice of four genotypes is shown; WT mice show a single band (465 bp) on the *Fmr1* gel and a single band (445 bp) on the *Grm5* gel; KO mice show a single band (800 bp) on the *Fmr1* gel and a single band (445 bp) on the *Grm5* gel; HT mice show a single band (465 bp) on the *Fmr1* gel and a double band (445 bp and 550 bp) on the *Grm5* gel; CR mice show a single band (800 bp) on the *Fmr1* gel and a double band (445 bp and 550 bp) on the *Grm5* gel. (C) Western blot analysis of total mGluR5 expression in visual cortical homogenates from P30 normalized to WT (+/+, +/Y) mice, KO (+/+, -/Y), HT (+/-, +/Y), and CR (+/-, -/Y) (n = 11 per genotype, ANOVA P < 0.0001). *Grm5* KO (-/-, +/Y) control sample was run 4 times (n = 1 animal) and normalized to age matched (postnatal day 45) WT. Representative blot is shown above. (D) Significant effect of mGluR5 gene dosage on LTD in *Fmr1* KO mice. *Top*: Representative fEPSPs from KO and CR recordings taken at times indicated below. Traces are average of 10 consecutive sweeps. *Bottom*: Time course of experimenter-blind experiments in which 50 μ M (RS)-3,5-dihydroxyphenylglycine (DHPG) was applied for 5 min (arrow) to slices from KO and CR animals (n = 14 and 11 slices from 6 and 5 mice for KO and CR, respectively). Multiple slices per animal were averaged together. Average field EPSP slopes 45-50 min after DHPG were significantly different from 5 min averages immediately prior to DHPG in both genotypes (% baseline: KO = 78.1 ± 3.1 %, P = 0.000005; CR = 91.6 ± 1.4 %, P = 0.00007; paired t-test). However, reduction of *Grm5* gene dosage by 50% significantly decreases magnitude of LTD in CR relative to *Fmr1* KO mice (n = 5 and 6 animals, respectively, P = 0.0058, unpaired t-test).

A

Parents (c57Bl/6J background):

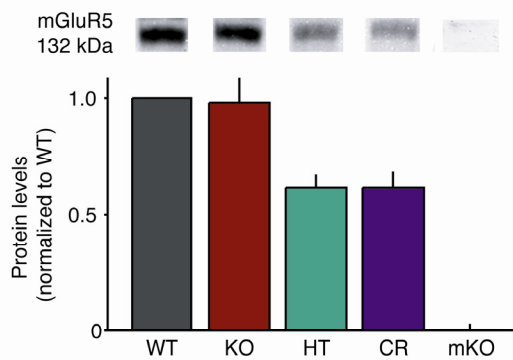
 $Fmr1$ HET ♀ X $Grm5$ HET ♂

♂ Offspring:

	XM	xM
YM	XYMM	xYMM
Ym	XYMm	xYMm

	WT (XYMM)	KO (xYMM)	HT (XYmM)	CR (xYmM)
<i>Fmr1</i>	+/Y	-/Y	+/Y	-/Y
<i>Grm5</i>	+/+	+/+	+/-	+/-

C



B

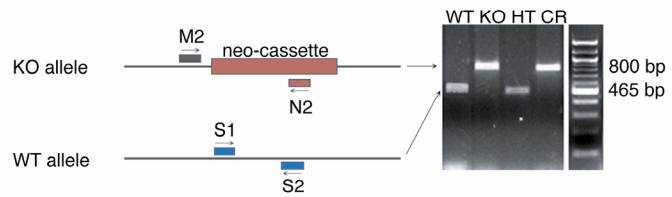
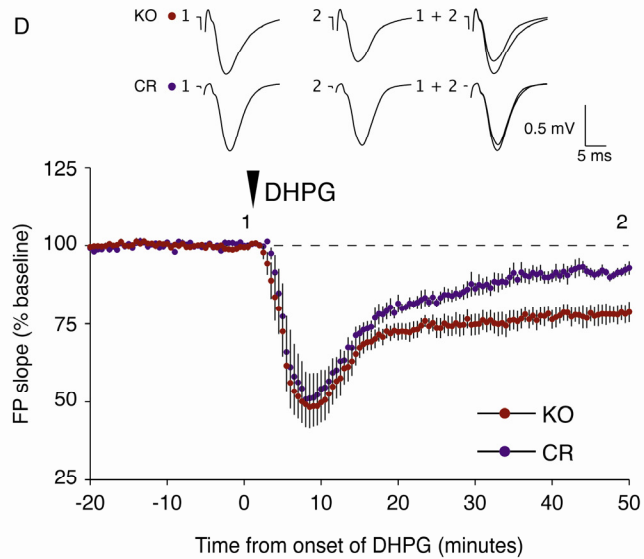
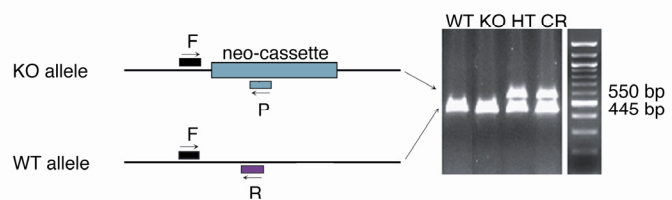
Fmr1 Locus on X Chromosome*Grm5* (mGluR5) Locus on Chromosome 7

Figure S3. Changes in VEP amplitude as a function of deprivation duration in WT mice

These data are re-plotted from Frenkel and Bear (2004). **(A)** MD of the contralateral eye in WT mice for 3 days induces statistically significant changes in contralateral-eye VEP responses (blue bars representing mean \pm SEM, $n = 15$). **(B)** 7 days of MD in WT mice induces statistically significant changes in contralateral and ipsilateral (yellow bars) VEP responses ($n = 17$) Post-hoc t-tests: * equals significantly different from baseline (day 0). **(C)** Data from animals in A and B are replotted using a plasticity index that indicates the fractional changes in contralateral and ipsilateral eye responses. Significant differences exist in the plasticity profile between 3 and 7 days MD (MANOVA 3d:7d $P = 0.020$).

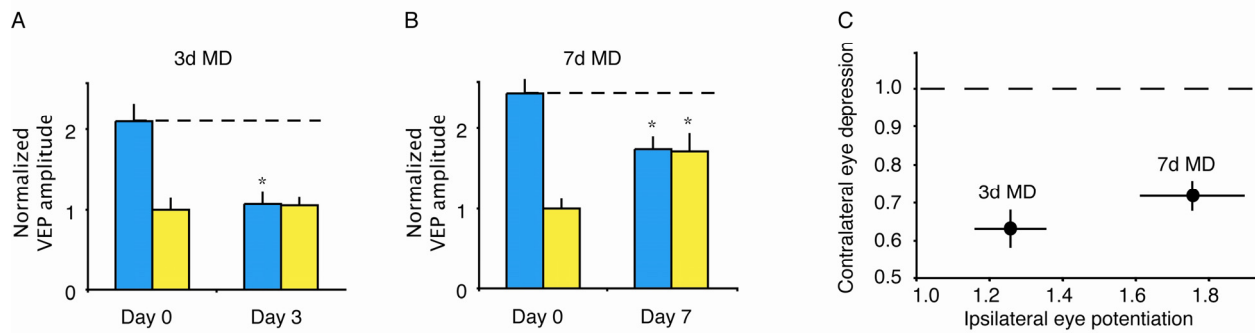


Figure S4. Genetic rescue of growth phenotype in FXS

(A) Photograph of littermate animals of four genotypes at P29. (B) Body weight data across four genotypes fitted to polynomial curves (C) Normal body weight (mean \pm SEM) across genotypes at weaning (P20) (WT n = 18, KO n = 23; HT n = 24; CR n = 16). Increased body weight in KO mouse at P26, rescued in CR, not different in HT (WT n = 36, KO n = 26, HT n = 20, CR n = 40). Maximal body weight increase in KO mouse at P30, rescued in CR, not different in HT (WT n = 17, KO n = 17, HT n = 10, CR n = 15). Body weight phenotype in KO is absent by P45 (WT n = 17, KO n = 17, HT n = 10, CR n = 15). Post-hoc t-tests: *indicates significantly different from WT, † indicates significantly different from KO.

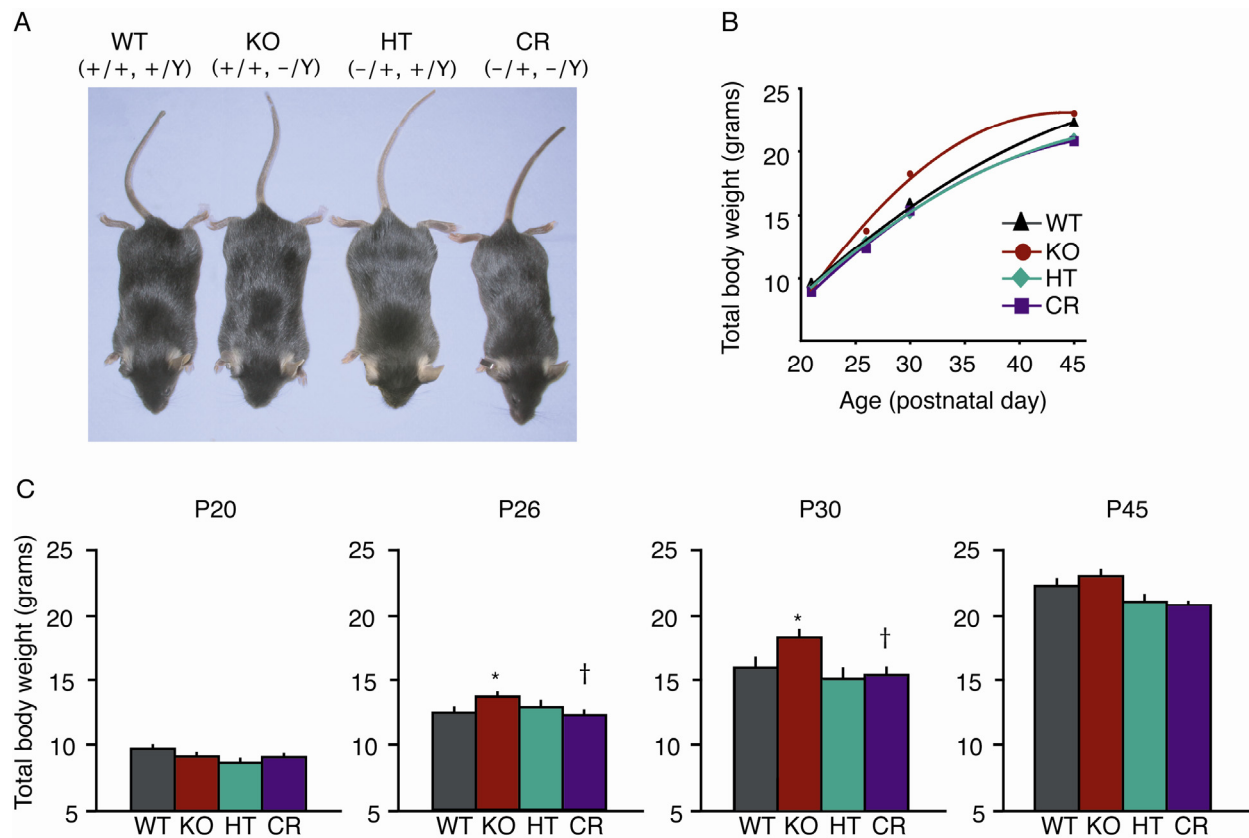


Figure S5. Macroorchidism phenotype is not rescued by reduction in mGluR5 gene dosage
(A) Testicular weights (mean \pm SEM) were not significantly different in juvenile mice across genotypes (P30). **(B)** Testicular weight differences across genotypes become evident in adulthood (average age P80). KO phenotype is not rescued in the CR mice or in dKO mice (WT n = 20, KO n = 14, HT n = 10, CR n = 10, mKO n = 7, dKO n = 6). Post-hoc t-tests: * indicates significantly different from WT, † indicates significantly different from KO.

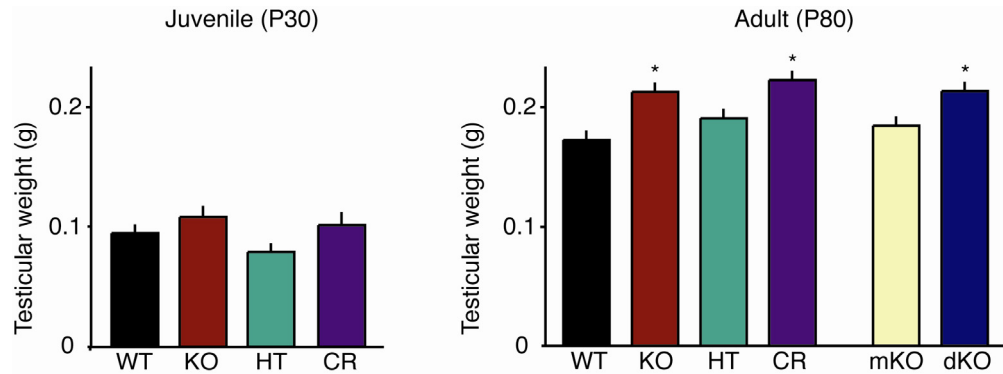


Table S1. Rescue of audiogenic seizure phenotype in FXS

Significant differences in AGS susceptibility exist across the four genotypes (WT n = 15, n = 18 KO, HT n = 19, CR n = 15). Mann-Whitney U: *indicates significantly different from WT, † indicates significantly different from KO. Cartoon modified from Raisinghani and Faingold, 2005.

	wild running	seizure (clonic/tonic)	status epilepticus	% incidence
WT	0/15	0/15	0/15	0.0%
KO	13/18	13/18	7/18	72.2% *
HT	0/19	0/19	0/19	0.0%
CR	5/15	5/15	2/15	33.3% * †